

## Azimuthal instability of spinning spatiotemporal solitons

D. Mihalache,<sup>1,2</sup> D. Mazilu,<sup>1,2</sup> L.-C. Crasovan,<sup>1,2</sup> B. A. Malomed,<sup>3</sup> and F. Lederer<sup>1</sup>

<sup>1</sup>*Institute of Solid State Theory and Theoretical Optics, Friedrich-Schiller University Jena, Max-Wien-Platz 1, D-07743, Jena, Germany*

<sup>2</sup>*Department of Theoretical Physics, Institute of Atomic Physics, P.O. Box MG-6, Bucharest, Romania*

<sup>3</sup>*Department of Interdisciplinary Sciences, Faculty of Engineering, Tel Aviv University, Tel Aviv 69978, Israel*

(Received 4 November 1999)

We find one-parameter families of three-dimensional spatiotemporal bright vortex solitons (doughnuts, or *spinning light bullets*), in dispersive quadratically nonlinear media. We show that they are subject to a strong instability against azimuthal perturbations, similarly to the previously studied (2+1)-dimensional bright spatial vortex solitons. The instability breaks the spinning soliton into several fragments, each being a stable nonspinning light bullet.

PACS number(s): 42.65.Tg, 42.65.Ky

Optical spatiotemporal solitons, or *light bullets* (LBs), have been attracting a growing interest in the last decade [1–16], as they are expected to be new fundamental physical objects with a potential for using them in ultrafast all-optical switching devices in planar and bulk media. It is well known that LBs formally exist in dispersive media with the self-focusing cubic (Kerr) nonlinearity, but, in both two- and three-dimensional (2D and 3D) cases, they are unstable against spatiotemporal collapse [11], induced by a combined effect of the nonlinearity and anomalous dispersion [3]. However, collapse does not take place, making stable LBs possible, in media with saturable [8–10], quadratic [12,13], and cubic-quintic [14] nonlinearities, in off-resonance two-level systems [15] as well as in self-induced-transparency media [16]. The second-harmonic generation (SHG) media are most appropriate for the experimental observation of LBs. Theoretical work in this direction, which had begun two decades ago [1] and continued recently [12,13], has led to the first experimental observation of optical spatiotemporal solitons [6]. In fact, the observed object was a 2D spatiotemporal soliton in a 3D sample of an optical crystal (i.e., it was localized in the longitudinal and one of transverse directions, but delocalized in the other transverse coordinate). It is also relevant to mention that, while a majority of works on LBs were dealing with solitons of the bright type, dark LBs were considered too [7].

In this Rapid Communication we aim to find numerically one-parameter families of 3D *spinning* (vortex) LBs in a model of a type-I SHG medium. The model assumes different coefficients of the group velocity dispersion (GVD) at the fundamental-frequency (FF) and second-harmonic (SH) waves [12], but neglects the Poynting-vector walkoff and temporal group-velocity mismatch. Spinning LBs in models of this type were recently introduced in a brief form in Ref. [17], using a variational approximation and very limited numerical computations. Nevertheless, a crucially important issue is the (in)stability of the spinning LBs against azimuthal perturbations, which will be considered in the present work.

It should be noted that azimuthal instability of 2D spinning solitons, which may also be interpreted as quasi-2D (cylindrical) solitons in a 3D medium, was studied in detail in the works in Ref. [18]. However, as was shown still in the early work [1], all the solitons of the cylindrical type in 3D SHG media are subject to modulational instability along the

cylindrical axis; therefore, it is an issue of principal interest to study fully localized 3D LBs, which may be naturally generated as a result of development of the modulational instability (similar to the generation of an array of spots by the snake-type modulational instability of a spatial soliton in a 2D SHG medium [19]).

The scaled equations describing type-I SHG processes (i.e., involving a single FF polarization) in the (3+1)D geometry in the presence of dispersion and diffraction are well known [12]:

$$i \frac{\partial u}{\partial Z} + \frac{1}{2} \left( \frac{\partial^2 u}{\partial X^2} + \frac{\partial^2 u}{\partial Y^2} + \frac{\partial^2 u}{\partial T^2} \right) + u^* v = 0, \quad (1)$$

$$i \frac{\partial v}{\partial Z} + \frac{1}{4} \left( \frac{\partial^2 v}{\partial X^2} + \frac{\partial^2 v}{\partial Y^2} + \sigma \frac{\partial^2 v}{\partial T^2} \right) - \beta v + u^2 = 0.$$

Here,  $T$  and  $X, Y$  are normalized temporal and transverse spatial coordinates,  $Z$  is the normalized propagation distance, and  $u, v$  are envelopes of the FF and SH fields. A phase mismatch between the two harmonics is  $\beta$ , and  $\sigma$  is the ratio of the GVD coefficients at the two frequencies. In the particular case  $\sigma=1$ , the model possesses an additional spatiotemporal spherical symmetry [12,13].

We look for stationary solutions to Eqs. (1) in the form  $u = U(r, T) \exp(i\kappa Z + is\theta)$ ,  $v = V(r, T) \exp[2(i\kappa Z + is\theta)]$ , where  $\theta$  is the polar angle in the transverse plane,  $\kappa$  is a wave number shift, and the integer  $s$  is the ‘‘spin.’’ The amplitudes  $U$  and  $V$  may be taken real, obeying the equations

$$\frac{1}{2} \left( \frac{\partial^2 U}{\partial r^2} + \frac{1}{r} \frac{\partial U}{\partial r} - \frac{s^2}{r^2} U + \frac{\partial^2 U}{\partial T^2} \right) - \kappa U + UV = 0, \quad (2)$$

$$\frac{1}{4} \left( \frac{\partial^2 V}{\partial r^2} + \frac{1}{r} \frac{\partial V}{\partial r} - \frac{4s^2}{r^2} V + \sigma \frac{\partial^2 V}{\partial T^2} \right) - (2\kappa + \beta) V + U^2 = 0.$$

In Eqs. (2),  $\sigma$  and  $\beta$  are material and carrier-wave parameters, while  $\kappa$  parametrizes the family of the stationary solutions. Note that solutions of this form assume that the phase helix is in the transverse spatial plane ( $X, Y$ ). One can also consider LBs with a phase helix in a spatiotemporal plane. In the general case,  $\sigma \neq 1$ , such solutions lack the axial symme-

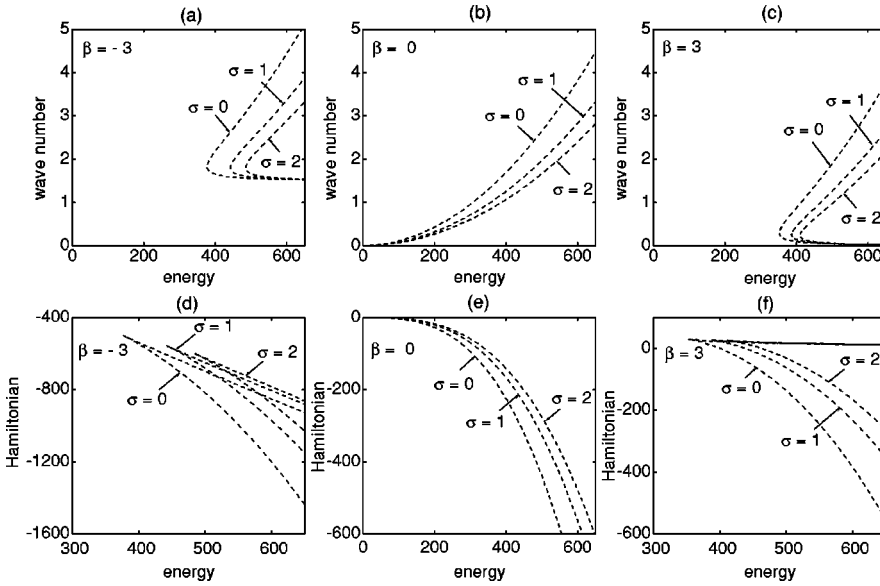


FIG. 1. Nonlinear wave number  $\kappa$  and Hamiltonian  $H$  vs the energy  $I$  for the light bullets with spin  $s = 1$ .

try; therefore, their analysis is much more complicated and is left beyond the scope of this work.

The total energy of LBs is  $I = \iint\iint (|u|^2 + |v|^2) dXdYdT \equiv I_u + I_v$ , which is a conserved quantity. The other dynamical invariants are the Hamiltonian  $H$ , the momentum (equal to zero for the solution considered here), and the angular momentum  $L$  in the transverse plane [20]. One can readily find from Eqs. (1) and (2) that the Hamiltonian and the angular momentum of stationary spinning LBs are related as follows:  $3H = -\kappa I + \beta I_v$ , and  $L = sI$ .

We have numerically found one-parameter families of stationary 3D spinning-LBs solutions which have the shape of a doughnut with a hole (phase dislocation) in the center, for different values of the GVD-asymmetry parameter  $\sigma$ . A standard band-matrix algorithm was used to deal with the corresponding two-point boundary-value problem.

It was found that solutions exist provided that their energy exceeds a certain *threshold*. At the exact phase-matching point ( $\beta = 0$ ), the threshold vanishes. For stationary solutions to decay exponentially at infinity, the wave number  $\kappa$  has to obey the requirements  $\kappa > 0$  for  $\beta \geq 0$ , or  $\kappa > -\beta/2$

for  $\beta < 0$ . We were able to find solitons only in the case when the SH dispersion is anomalous or zero,  $\sigma \geq 0$ .

To characterize the LB solutions, in Fig. 1 we display the wave number  $\kappa$  and the Hamiltonian  $H$  of spinning LBs with  $s = 1$  versus its net energy  $I$  for three representative values of the mismatch  $\beta$  and for various values of the GVD-asymmetry parameter  $\sigma$ . For larger values of the ‘‘spin’’ (e.g.,  $s = 2$ ), the results are similar, although the threshold energies are higher (see Fig. 2). In Fig. 3 we plot the curves  $\kappa = \kappa(I)$  and  $H = H(I)$  for *both* nonspinning and spinning LBs with  $\sigma = 2$  and three values of  $\beta$ . Solid and dashed lines correspond, respectively, to the branches which are, respectively, stable and unstable against azimuthal perturbations (in fact, only the zero-spin solutions are stable). To conclude the discussion of the stationary solutions, we note that a comparison with the simple variational approximation for the spinning LBs, briefly described in Ref. [17], demonstrates that, although the variational approximation is not very accurate, it correctly describes qualitative features of the shape of the spinning LBs.

Proceeding to the stability simulations, we solved Eqs.

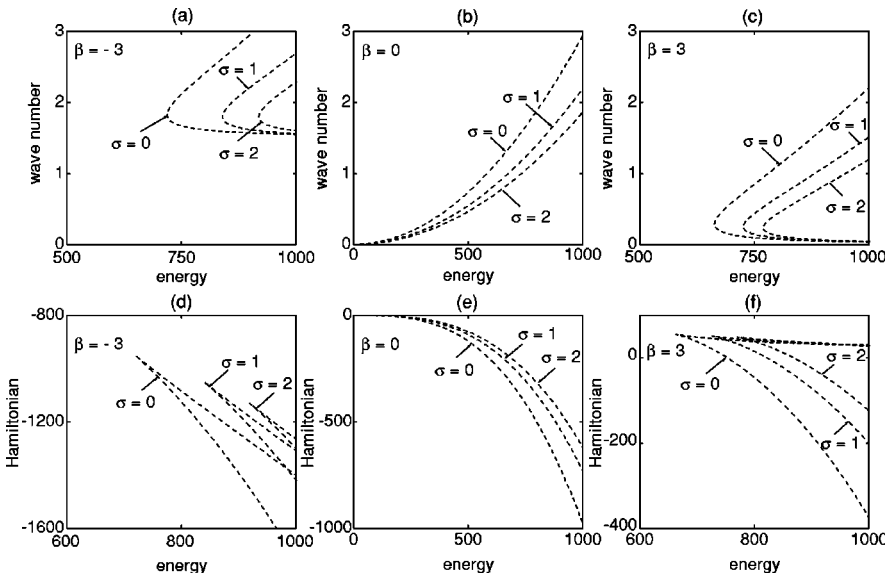


FIG. 2. The same as in Fig. 1 for  $s = 2$ .

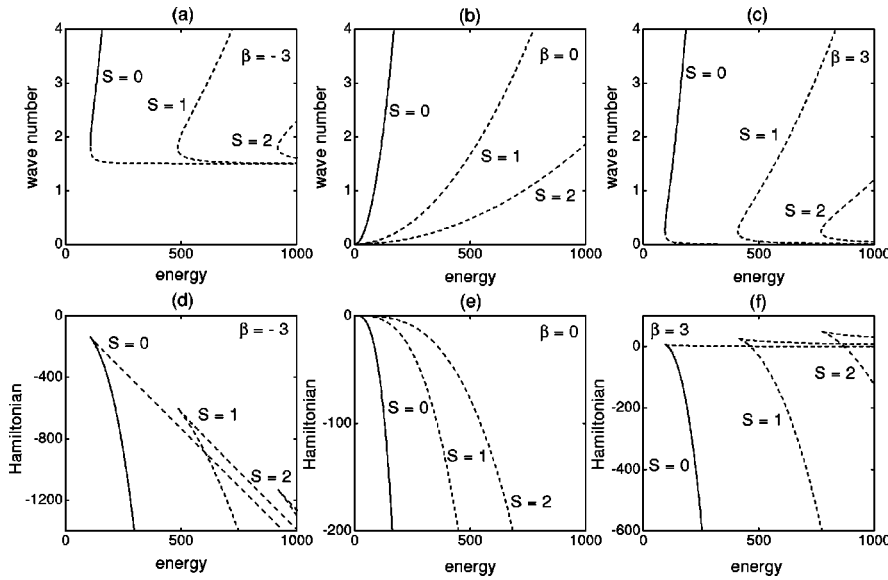


FIG. 3. Comparison between dependences of the wave number  $\kappa$  and Hamiltonian  $H$  on the energy  $I$  for the nonspinning ( $s = 0$ ) and one-ring (fundamental) spinning ( $s = 1$  and  $s = 2$ ) light bullets. In this figure,  $\sigma = 2$ .

(1), using the Crank-Nicholson scheme. The corresponding system of nonlinear equations was solved by means of the Picard iteration method, and the resulting linear system was treated by means of the Gauss-Seidel iterative scheme. For good convergence we needed, typically, five Picard iterations and eight Gauss-Seidel iterations. The transverse grid step sizes were  $0.08 \leq \Delta X = \Delta Y = \Delta T \leq 0.12$  and, in most cases, the longitudinal step size was  $\Delta Z = 0.01$ . To avoid distortion of the instability development under the action of the periodicity imposed by the Cartesian computational mesh, we added initial perturbations that mimic random fluctuations in a real system (cf. Ref. [21]). Figures 4 and 5 display the outcome of numerical simulations: the doughnutlike spinning LBs are *always* unstable against azimuthal perturbations, which lead to the breakup of the doughnuts into several *nonspinning* LBs. In fact, this instability is quite similar to the theoretically [18] and experimentally [22] known instability of (2+1)D one-ring (fundamental) and two-ring (second-order) spatial bright vortex solitons in saturable and quadratically nonlinear media. It is also noteworthy that higher-order nonspinning solitary waves in saturable media exhibit similar transverse instabilities that break their azimuthal symmetry [21,23]. Examples of the breakup of the one-ring spinning LBs with  $s = 1$  and  $s = 2$  are displayed in Fig. 4. Three emerging fragments were found to have unequal energies in the  $s = 1$  case, whereas four fragments are found to have exactly equal energies in the  $s = 2$  case. After the breakup of the doughnut, the fragments fly out tangentially, rather than keeping to spiral [similar to what is known about the instability-induced breakup of the (2+1)D spatial vortex solitons [18]]. This feature is illustrated by Fig. 5, in which a succession of images at different values of  $Z$  [ $7.5 \leq Z \leq 9$  in (a) and  $4.2 \leq Z \leq 8.2$  in (b)] are juxtaposed. Thus, the initial angular momentum of the doughnut-shaped “spinning” soliton is converted into the angular momenta of the emerging nonspinning fragments. Last, we have found that the number of the emerging fragments is roughly twice the original spin value  $s$ . The dependence of the number of the fragments on the other parameters is fairly weak.

The results of direct dynamical simulations reported in this work must comply with the stability analysis based on

Eqs. (1) linearized around of the stationary spinning LBs. In particular, similar to Refs. [18,23], we expect that the number of the emerging fragments is determined by the azimuthal index of the perturbation mode having the largest growth rate. However, the corresponding eigenvalue problem turns out to be prohibitively complex; therefore, its solution is left beyond the scope of this work.

Recently, spinning 3D LBs were also studied in detail in the cubic-quintic model [14], and their stability was tested in direct simulations [24]. As a result, it has been found that the doughnut spatiotemporal solitons are always azimuthally unstable in this model too. Nevertheless, in some cases (when the soliton’s energy is large enough), this instability may be much weaker than that found in the present work for SHG nonlinearity. In fact, spinning solitons in the cubic-quintic model may have a chance to be observed in an experiment as virtually stable objects [24].

To create spinning solitons in the experiment, one can

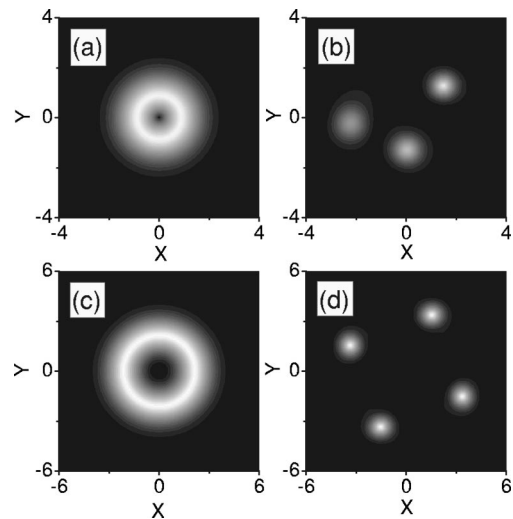


FIG. 4. Gray-scale contour plots illustrating the instability of the one-ring spinning light bullets. In (a) and (b)  $s = 1, \kappa = 3$  while in (c) and (d)  $s = 2, \kappa = 2.2$ . The other parameters are  $\sigma = 2$  and  $\beta = -3$ . The propagation distance is  $Z = 8$  for  $s = 1$ , and  $Z = 7$  for  $s = 2$ . Only the fundamental-frequency component is shown.

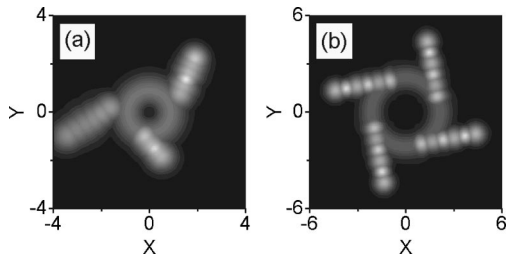


FIG. 5. Juxtaposed images showing trajectories of the nonspinning fragments flying out after the breakup of the spinning light bullet. In (a)  $s=1$ , and in (b)  $s=2$ . The other parameters are the same as in Fig. 4. Only the fundamental-frequency component is shown.

give the necessary vorticity to a short cylindrical laser pulse, passing it through a properly fabricated phase mask [22]. To estimate real physical parameters at which the spinning LBs and their instability can be observed in the experiment (similar to the experimental observation of the instability of the spatial vortex bright solitons in Ref. [22]), we can use the parameters at which the 2D spatiotemporal solitons in the SHG media were recently observed in Refs. [6]. In the  $\text{LiIO}_3$  optical crystal (in which the necessary temporal dispersion is induced artificially, by means of a grating), the light with the intensity  $\sim 10 \text{ GW/cm}^2$  self-traps into a spatiotemporal soliton with characteristic temporal and spatial sizes  $\sim 100 \text{ fs}$  and  $40 \mu\text{m}$ , respectively. In the case of the 3D LB, the intensity should be, roughly, twice as large (see Ref. [12]). Next, Fig. 3 shows that, for the spinning LB with  $s=1$ , the energy is, typically, five times as large as for the zero-spin soliton with the same size (quite a similar conclu-

sion about the ratio of the energies in the cubic-quintic model was obtained in Ref. [14]). Thus, we arrive at an estimate for the energy of the spinning 3D LB of about  $1 \mu\text{J}$ . These values of the physical parameters suggest that the experiment aimed to observe 3D LBs should be quite feasible.

For the physical interpretation of the results, it is also important to understand the real meaning of the propagation distances that appear in the above figures. A typical size of the  $s=1$  LB is, in the dimensionless units,  $\Delta x \sim 2$ ; hence, the corresponding diffraction length is  $z_D \sim (\Delta x)^2 \sim 4$ . Thus, the comparison with Fig. 4 and with other numerical results suggests that the full splitting of the spinning LB takes place within a few diffraction lengths. On the other hand, a typical value of  $z_D$  in physical units is  $\sim 3-5 \text{ mm}$  (for the FF wave) [6]. This shows that the splitting process may be observed in available samples having lengths up to  $25 \text{ mm}$  [6].

In conclusion, in the framework of the standard model of the type-I second-harmonic generation in a three-dimensional dispersive medium, we have found numerically one-parameter families of spatiotemporal doughnut-shaped spinning (vortex) solitons. All the spinning solitons show a strong symmetry-breaking azimuthal instability. The instability splits the spatiotemporal soliton into stable zero-spin light bullets (at least three), which fly out tangentially to the initial ring.

D. Mihalache, D. Mazilu, L.-C. Crasovan, and F. Lederer acknowledge grants from the Deutsche Forschungsgemeinschaft (DFG), Bonn (Grant No. SFB 196), and B. Malomed appreciates the hospitality of the University of Jena. We are indebted to Frank Wise for valuable discussions and for sending us his work prior to publication.

- 
- [1] A. A. Kanashov and A. M. Rubenchik, *Physica D* **4**, 122 (1981).
- [2] J. T. Manassah, P. L. Baldeck, and R. R. Alfano, *Opt. Lett.* **13**, 1090 (1988).
- [3] Y. Silberberg, *Opt. Lett.* **15**, 1282 (1990).
- [4] A. B. Blagoeva, S. G. Dinev, A. A. Dreischuh, and A. Naidenov, *IEEE J. Quantum Electron.* **QE-27**, 2060 (1991).
- [5] K. Hayata and M. Koshihba, *Phys. Rev. Lett.* **71**, 3275 (1993); *Phys. Rev. E* **48**, 2312 (1993).
- [6] X. Liu, L.J. Qian, and F. W. Wise, *Phys. Rev. Lett.* **82**, 4631 (1999); X. Liu, K. Beckwitt, and F. Wise, *Phys. Rev. E* **61**, R4722 (2000).
- [7] Y. Chen and J. Atai, *Opt. Lett.* **20**, 133 (1995).
- [8] R. H. Enns, D. E. Edmundson, S. S. Rangnekar, and A. E. Kaplan, *Opt. Quantum Electron.* **24**, S1295 (1992).
- [9] D. E. Edmundson and R. H. Enns, *Phys. Rev. A* **51**, 2491 (1995); *Opt. Lett.* **18**, 1609 (1993).
- [10] R. McLeod, K. Wagner, and S. Blair, *Phys. Rev. A* **52**, 3254 (1995).
- [11] L. Bergé, V. K. Mezentsev, J. J. Rasmussen, and J. Wyller, *Phys. Rev. A* **52**, R28 (1995); L. Bergé, O. Bang, J. J. Rasmussen, and V. K. Mezentsev, *Phys. Rev. E* **55**, 3555 (1997).
- [12] B. A. Malomed, P. Drummond, H. He, A. Berntson, D. Anderson, and M. Lisak, *Phys. Rev. E* **56**, 4725 (1997); D. Mihalache, D. Mazilu, B. A. Malomed, and L. Torner, *Opt. Commun.* **152**, 365 (1998); **169**, 341 (1999); D. Mihalache, D. Mazilu, J. Dörring, and L. Torner, *ibid.* **159**, 129 (1999).
- [13] D. V. Skryabin and W. J. Firth, *Opt. Commun.* **148**, 79 (1998).
- [14] A. Desyatnikov, A. I. Maimistov, and B. A. Malomed, *Phys. Rev. E* **61**, 3107 (2000).
- [15] I. V. Mel'nikov, D. Mihalache, and N.-C. Panoiu, *Opt. Commun.* **181**, 345 (2000).
- [16] M. Blaauboer, B. A. Malomed, and G. Kurizki, *Phys. Rev. Lett.* **84**, 1906 (2000).
- [17] Y. Bakman and B. Malomed, in *Nonlinear Guided Waves and Their Applications*, OSA Technical Digest (Optical Society of America, Washington DC, 1999), p. 389.
- [18] W. J. Firth and D. V. Skryabin, *Phys. Rev. Lett.* **79**, 2450 (1997); D. V. Petrov and L. Torner, *Opt. Quantum Electron.* **29**, 1037 (1997); D. V. Skryabin and W. J. Firth, *Phys. Rev. E* **58**, 3916 (1998).
- [19] A. De Rossi, S. Trillo, A.V. Buryak, and Y.S. Kivshar, *Opt. Lett.* **22**, 868 (1997).
- [20] N. N. Akhmediev and A. Ankiewicz, *Solitons: Nonlinear Pulses and Beams* (Chapman and Hall, London, 1997).
- [21] D. E. Edmundson, *Phys. Rev. E* **55**, 7636 (1997); see also <http://www.sfu.ca/~renns/lbullets.html>.
- [22] D. V. Petrov, L. Torner, J. Martorell, R. Vilaseca, J. P. Torres, and C. Cojocaru, *Opt. Lett.* **23**, 1444 (1998).
- [23] J. M. Soto-Crespo, D. R. Heatley, E. M. Wright, and N. N. Akhmediev, *Phys. Rev. A* **44**, 636 (1991); J. Atai, Y. Chen, and J. M. Soto-Crespo, *ibid.* **49**, R3170 (1994).
- [24] D. Mihalache, D. Mazilu, L.-C. Crasovan, B. A. Malomed, and F. Lederer, *Phys. Rev. E* **61**, 7142 (2000).